DOI: 10.3969/j.issn.1673-3185.2017.02.009 **http:** // english.ship-research.com

Translated from: ZHOU Y M, ZHANG S Y, LU W, et al. High-efficiency airfoil rudders applied to submarines[J]. Chinese Journal of Ship Research, 2017, 12(2): 71-77.

High-efficiency airfoil rudders applied to submarines

ZHOU Yimei, ZHANG Shuyi, LU Wei, HE Hanbao

China Ship Development and Design Center, Wuhan 430064, China

Abstract: Modern submarine design puts forward higher and higher requirements for control surfaces, and this creates a requirement for designers to constantly innovate new types of rudder so as to improve the efficiency of control surfaces. Adopting the high-efficiency airfoil rudder is one of the most effective measures for improving the efficiency of control surfaces. In this paper, we put forward an optimization method for a high-efficiency airfoil rudder on the basis of a comparative analysis of the various strengths and weaknesses of the airfoil, and the numerical calculation method is adopted to analyze the influence rule of the hydrodynamic characteristics and wake field by using the high-efficiency airfoil rudder and the conventional NACA rudder comparatively; at the same time, a model load test in a towing tank was carried out, and the experimental results and simulation calculation obtained good consistency: the error between them was less than 10%. The experimental results show that the steerage of a high-efficiency airfoil rudder is increased by more than 40% when compared with the conventional rudder, but the total resistance is close: the error is no more than 4%. Adopting a high-efficiency airfoil rudder brings much greater lifting efficiency than the total resistance of the boat. The results show that high-efficiency airfoil rudder has obvious advantages for improving the efficiency of control, giving it good application prospects.

Key words: submarine; high-efficiency airfoil rudder; hydrodynamic characteristics; wake field

CLC number: U661.33

0 Introduction

With the development of submarine technology, the requirement of control surface design is increasingly higher. First of all, the tonnage of conventional submarine is larger and larger, and limited by ultra-wide and ultra-baseline control surface, it is more and more difficult to meet the requirements for the index of maneuverability such as climbing rate, so there is an urgent need to improve the control surface efficiency to ensure the maneuverability of submarine. Secondly, the development of the stealth performance of submarine also puts forward higher and higher requirements for the design of control surface. In order to achieve the goal of quiet submarine, navies of China and abroad have been studying the vibration and noise reduction technology for submarines, including research on reducing the hydrodynamic noise, but it also puts forward higher requirements for the research and design of control surface. For example, the stern control surface is demanded to be as far as possible away from the propeller disk to reduce the influence of propeller wake field; the acoustic target strength is decreased by reducing the control surface area; the vibration is reduced by controlling the span of control surfaces. The restriction of these factors makes the maneuverability design more and more difficult, and it is necessary for designers to try to study the new rudder types to improve the efficiency of the control surfaces[1].

One of the measures to improve the efficiency of airfoil is the use of high-efficiency airfoil profile[2]. When high-efficiency airfoil profile is applied to submarine, in addition to obtain good steerage, the resistance cannot be increased too much. The propeller noise cannot be obviously affected when high-efficiency airfoil profile is applied to the stern rudder. In order to solve this problem, this paper will study

Received: 2016-08-29

Author(s): ZHOU Yimei (Corresponding author), female, born in 1972, master, senior engineer. Research interest: ship maneuverability

the application of high-efficiency airfoil rudder in submarine.

1 High-efficiency airfoil rudder profile scheme

1.1 Common forms of airfoil profile

In order to improve the hydrodynamic performance of rudder, scholars of hydromechanics in China and abroad have done a lot of research on the airfoil profile, and published a lot of papers about the rudder profile forms and hydrodynamic force. In foreign countries, the relatively well-known are as follows: NACA series of National Advisory Committee for Aeronautics, the Joukowsky НЕЖ series of the Krylov Institute of the former Soviet Union, the ЦАГЙ series of the Aerodynamic Center Laboratory of the former Soviet Union, the Gottigen series of the Gottingen Laboratory and Jfs series of Hamburg Shipbuilding Institute (Taylor tank).

In China, the JDYW airfoil profile[3], which has high efficiency and good hydrodynamic characteristics, has been improved and optimized from many Chinese and foreign airfoils by Shanghai Jiao Tong University, and applied research has been carried out on a certain type of warship. The captive model experimental results show that under the same area and aspect ratio, stall angle of the JDYW airfoil profile was not less than that of the original NACA rudder, the noise was not greater than that of the original NACA rudder, but the relative turning diameter *D/L* at full rudder was reduced by 28.5% compared with the NACA rudder.

The fishtail rudder (or "contra rudder") developed by Wuhan University of Technology can make the lift coefficient increase by 1.5 times compared with the original NACA rudder[4]. Under the same rudder area, maneuvering performance of the contra rudder is better than that of the conventional NACA rudder. The results of the self-propelled model experimental also show that the turning diameter of the contra rudder at full rudder is 25.7% smaller than that of the conventional NACA rudder. Yu[5] and Yang[6] also carried out calculation and analysis on the hydrodynamic performance of fishtail rudder.

In these profile forms, NACA series have the most complete information and better comprehensive performance, which are still widely used today; the НЕЖ series also have better performance, but the single trailing edge is sharp and not practical; the JFS series have very high steerage, so is the WZF series developed based on the Schilling rudder of Germany, but the upper and lower swash plates must be configured, otherwise the second half strength will be slightly insufficient. Among them, profile forms of JFS and WZF series have 3 common characteristics: (1) the largest airfoil profile is closer to the bow edge thus to form the obtuse bow edge; (2) the trailing edges are both square edges; (3) shrinkage of the maximum profile to the trailing edge is large, and the straight section emerges.

Because these geometric features increase the profile curvature and change the pressure distribution of airfoil, an effect that increases the normal force of rudder is generated, resulting in a substantial increase in steerage. But there is a problem that because the rudderstock is installed near the maximum profile, and the maximum profile is too close to the bow edge, the rudder's balance ratio is too small. On the basis of the analysis of 4 excellent symmetrical airfoils (NACA series, НЕЖ series, JFS series and WZF series), JDYW symmetrical airfoil is designed by Shanghai Jiao Tong University. The above 5 types of rudder profiles are shown in Fig. 1. A rectangular balanced rudder with a normal aspect ratio of 1.5 and a thickness ratio of 0.18 was taken as an example, and the comparison of the efficiency of the 5 airfoil profiles is shown in Table 1[3], where t in the table is the thickness of a rudder, and b is the board length of a single rudder.

It can be seen from Table 1, the steerage of JDYW series was 45% higher than that of NACA series, 2% higher than that of WZF series, hence a good airfoil. Therefore, research of submarine airfoil profile in this paper will be carried out on this basis.

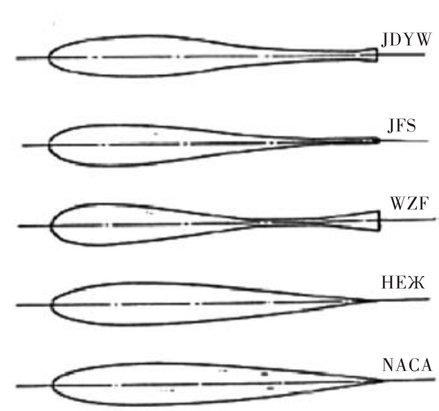

Fig.1 Five kinds of airfoil profile form

Table 1 The steerage of five kinds of excellent rudder types

Rudder type	Aspect ratio λ	Thickness ratio t/b	Shape	Test $Re(\times 10^5)$	Steerage CN_α	Comparison with NACA
JDYW	1.5	0.18	Rectangle, balanced	1.98	3.446 5	1.45
NACA	1.5	0.18	Rectangle, balanced	1.98	2.377 7	1.00
НЕЖ	1.5	0.18	Rectangle, balanced	1.98	3.064 9	1.29
JFS_{62TR25}	1.5	0.18	Rectangle, balanced	1.98	3.170 2	1.33
WZF	1.5	0.18	Rectangle, balanced	1.98	3.403 3	1.43

1.2 Airfoil profile scheme

In order to facilitate the comparison and analysis, 3 kinds of profile schemes were selected in this paper: NACA airfoil profile, JDYW profile and optimized high-efficiency airfoil profile. High-efficiency airfoil profile combines the advantages of airfoil profiles of JDYW and WZF series. The airfoil was set as fishtail, and the transitivity of the fishtail line was optimized, so as to improve the rationality of the use of steering engine power, and to increase the steerage to the maximum.

The comparison of the forms and values of the 3 profiles is shown in Fig. 2 and Fig. 3.

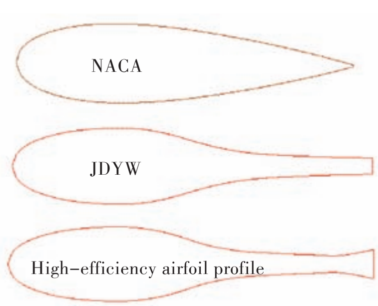

Fig.2 Three kinds of profile form in the numerical calculation

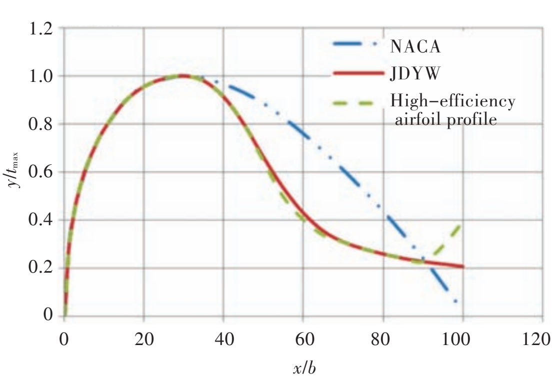

Fig.3 The comparison of three kinds of profile form

2 Comparative analysis of hydrodynamic characteristics of open water rudder

In the numerical calculation of open water rudder, Ma and Li et al.[7-9] have done a lot of research. Experience shows that better calculation accuracy can be obtained using the SIMPLEC algorithm combining RNG $k-\varepsilon$ turbulence model to calculate Reynolds-Averaged Navier-Stokes (RANS) equation. The pressure equation is discretized by a standard discrete scheme, and the momentum equation, turbulence equation and Reynolds stress equation are discretized by second-order upwind scheme. The mesh is structured, and in order to simulate the flow near the wall, the mesh is arranged reasonably in the boundary layer region and the suitable mesh scale is selected.

2.1 Computational domain and boundary conditions

The computational domain of a single rudder is shown in Fig. 4. The computational domain is a 5b long, 10 t_{max} high (t_{max} is the maximum thickness of a single rudder) rectangle that surrounds the flap type rudder, and the rectangular center axis and the symmetric axis of the rudder model are coincided; inflow boundary surface is the rectangular front face, 1b from the model head; outflow boundary surface is a rectangular rear end, 3b from the model tail; the outer boundary is 4 sides of the rectangle.

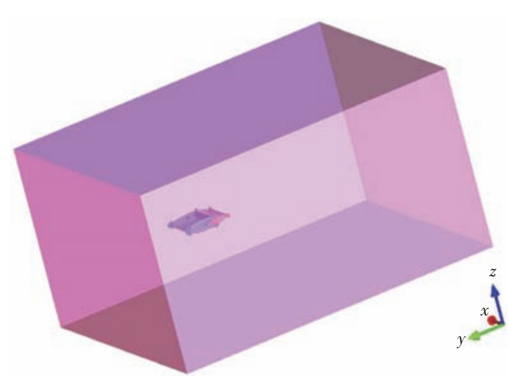

Fig.4 The computational domain area of the single rudder model

The boundary conditions are as follows:

1) Velocity inlet: at 1b forward from rudder head, the size and direction of the inflow velocity were set, and $\boldsymbol{V}_{in}=\boldsymbol{V}_0$; the turbulent kinetic energy and dissipation rate of turbulent kinetic energy at the inlet were determined by empirical formulas as follows: $k_{in}=3.75\times 10^{-3}\boldsymbol{V}_0^2$, $\varepsilon_{in}=k^{3/2}/0.03$.

2) Pressure outlet: at 3b backward from rudder tail, it was considered that the flow has been fully developed, so pressure outlet was used as boundary conditions.

3) Wall: that is, the outer surface of a single rudder. The non-slip conditions were set, $u=v=w=0$ (u, v, and w are respectively the longitudinal, transverse and vertical velocities).

4) External field: because the outer surface of the flow area was far enough away from the rudder, it was considered that there is no normal velocity on the surface. Thus, velocity inlet can be selected as boundary conditions.

2.2 Rudder surface pressure distribution

Rudder surface pressure distribution with the inflow velocity of 6 kn, the rudder angles of 0°, 5°, 10°, 15°, 20°, 25°, 30°, 35° were calculated. Fig. 5 and Fig. 6 are rudder surface pressure distribution contours of optimized high-efficiency airfoil rudder at 15° rudder angle.

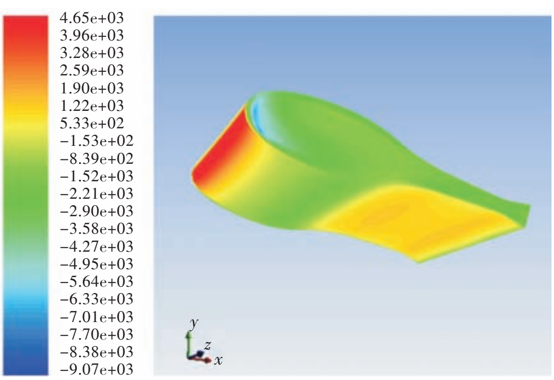

Fig.5 The inflow surface pressure contours of the high-efficient airfoil rudder

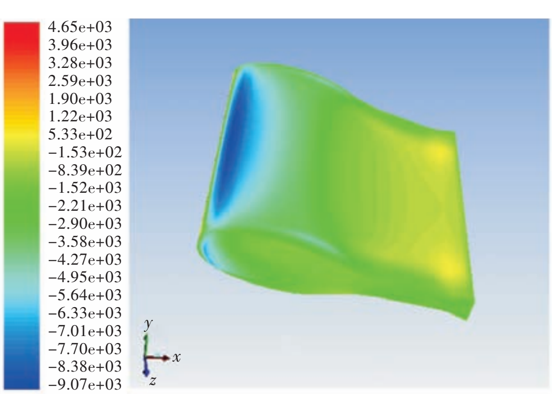

Fig.6 The back flow surface pressure contours of the high-efficient airfoil rudder

2.3 Hydrodynamic characteristics of the single rudder of three rudder types

The resistance coefficient, lift coefficient and pressure center coefficient of the 3 kinds of rudder types are compared by numerical calculation, as shown in Fig. 7 to Fig. 9.

It can be seen from the figures:

1) When the lift increases greatly, the resistance of the single rudder also increases greatly, and the increase of lift and resistance of the high-efficiency airfoil rudder is larger than that of the JDYW rudder. Compared with the NACA rudder, the resistance of the high-efficiency airfoil rudder was increased by 30%-40%, and the lift was increased by about 30% when the rudder angle was small, and it was increased by about 60% when the rudder angle was large.

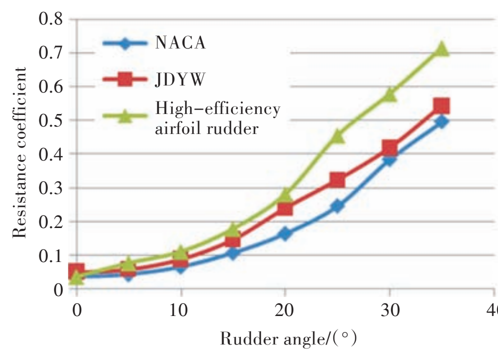

Fig.7 The comparison of resistance coefficients

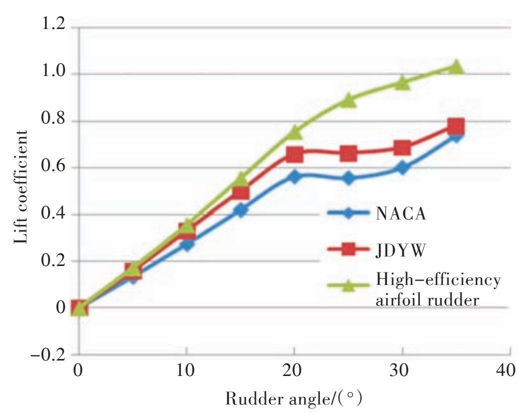

Fig.8 The comparison of lift coefficients

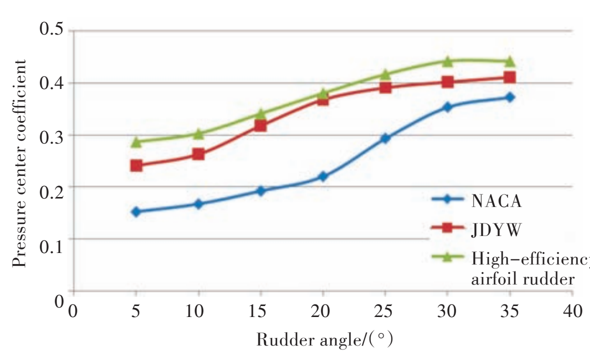

Fig.9 The comparison of pressure center coefficients

2) There is a significant difference in the pressure center coefficients between the 3 rudder types. Com-

pared with the NACA rudder, the pressure center coefficient of the high-efficiency airfoil rudder moved backwards, and the change with rudder angle was flat, which can be more beneficial to the rudder axis settings.

3 Comparative analysis of hydrodynamic characteristics of submarine rudder

The comparative analysis of the hydrodynamic characteristics of submarine rudder was carried out between the NACA rudder and the optimized high-efficiency rudder.

3.1 Computational domain and boundary conditions

The computational domain is shown in Fig. 10. The computational domain is a cylinder of $5L$ in length (L is the submarine length) and $10B$ in diameter (B is the submarine width) surrounding the submarine. The axis and the symmetric axis of the submarine model are coincided. The inflow boundary surface is the front face of the cylinder, $1L$ from the model head, and the outflow boundary surface is the rear face of the cylinder, $3L$ from the tail of the model; and the outer boundary is the cylindrical side.

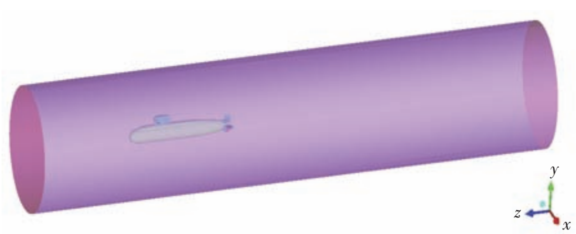

Fig.10 The computational domain of the submarine model

The boundary conditions are as follows:

1) Velocity inlet: at $1L$ forward from submarine bow, the size and direction of the inflow velocity were set, and $\boldsymbol{V}_{in} = \boldsymbol{V}_0$; the turbulent kinetic energy and dissipation rate of turbulent kinetic energy at the inlet were determined by empirical formulas as follows: $k_{in} = 3.75 \times 10^{-3} \boldsymbol{V}_0^2$, $\varepsilon_{in} = k^{3/2}/0.03$.

2) Pressure outlet: at $3L$ backward from the submarine stern, it was considered that the flow has been fully developed, so the pressure outlet was used as boundary conditions.

3) Wall: at the outer surface of the submarine, non-slip conditions were set, $u = v = w = 0$.

4) External field: because the outer surface of flow area was far enough away from the hull, it was considered that there was no normal velocity in the plane. Thus, velocity inlet can be taken as the boundary conditions.

3.2 Calculation and analysis of the influence of the two kinds of rudder on the resistance and yaw force

Based on the above numerical calculation, the influences of 2 kinds of rudder on the resistance and yaw force are shown in Fig. 11 and Fig. 12.

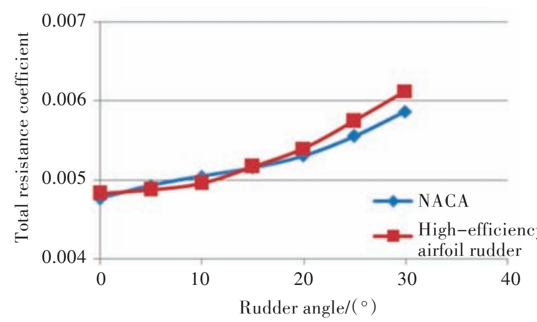

Fig.11 The comparison of total resistance coefficients

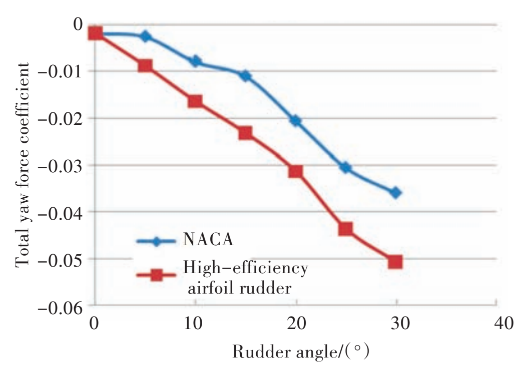

Fig.12 The comparison of total yaw force coefficients

From Fig. 11 and Fig. 12 it can be seen that at small rudder angle, the resistance increase of high-efficiency airfoil rudder and NACA rudder was almost the same. At 30° rudder angle, the resistance increase of high-efficiency airfoil rudder was 4.43% larger than that of NACA rudder; while compared with NACA rudder, the yaw force of the high-efficiency airfoil rudder increased very much, which was especially obvious at small rudder angle. At 30° rudder angle, the increase of yaw force was 41.23% larger than that of NACA rudder. The reason is that the rudder resistance is only a small proportion of the total resistance, and the rudder yaw force is the main component of yaw force that causes loofing. Thus, the lifting efficiency brought by the high-efficiency airfoil rudder is much greater than the effect of the total resistance on the hull.

4 Comparative analysis of model experimental results and simulation results

In order to verify the accuracy of the calculation results, a model load test of the open water rudder and the submarine rudder was carried out in the towing tank. The experimental model is shown in Fig. 13.

Fig.13 The experimental model

4.1 Open water experiment

The comparison between the numerical results and the experimental results of the open water experiment is shown in Fig. 14 and Fig.15.

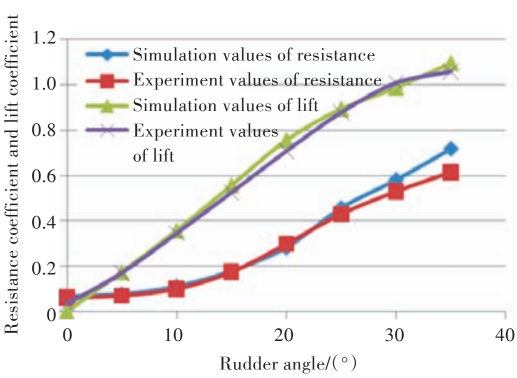

Fig.14 The comparison between simulation values and experiment values for resistance coefficient and lift coefficient of the high-efficiency airfoil rudder

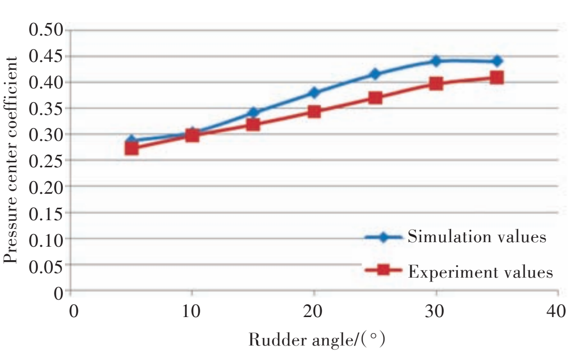

Fig.15 The comparison between simulation values and experiment values for pressure center coefficient of the high-efficiency airfoil rudder

As can be seen from the figures, the calculated values and the experimental values have consistent law, and the error between the lift calculation and model experiment is basically less than 10%.

4.2 Loofing experiment

Comparison between the experimental results and calculated results of high-efficiency airfoil rudder's loofing is shown in Fig. 16 and Fig. 17.

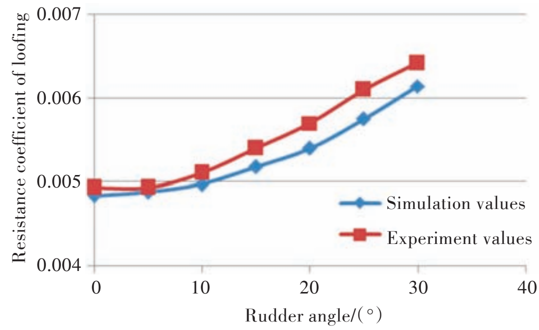

Fig.16 The comparison between simulation values and experiment values for resistance coefficient of the high-efficiency airfoil rudder's loofing

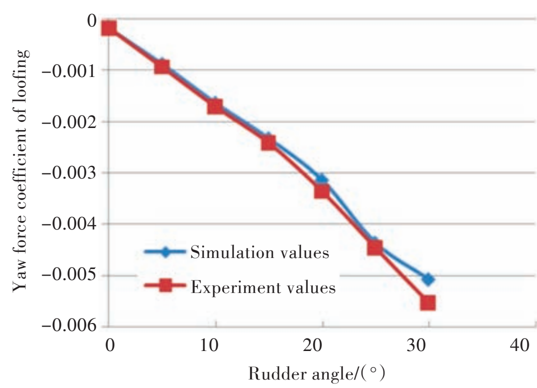

Fig.17 The comparison between simulation values and experiment values for yaw force coefficient of the high-efficiency airfoil rudder's loofing

As can be seen from the figures, the results of the numerical calculation and the model experiment are in good agreement, and the error is less than 10%, verifying the rationality of the law obtained by numerical simulation.

5 Analysis of the influence of high-efficiency airfoil rudder on wake field

Fig. 18 to Fig. 22 show the wake condition of the conventional cruciform rudder and the high-efficiency airfoil rudder at 10° rudder angle. In the figures: V_θ/V is the wake; θ is the circumferential angle; and R is the propeller radius. The wake is taken on the propeller disk surface, and the radii are taken as $0.4R$, $0.6R$, $0.8R$, $1.0R$ and $1.2R$ respectively.

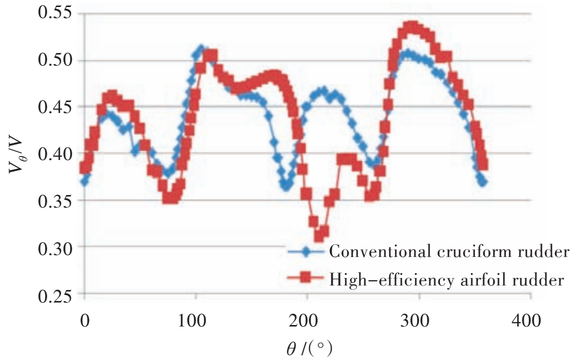

Fig.18 The comparison of wake at the radius of 0.4R

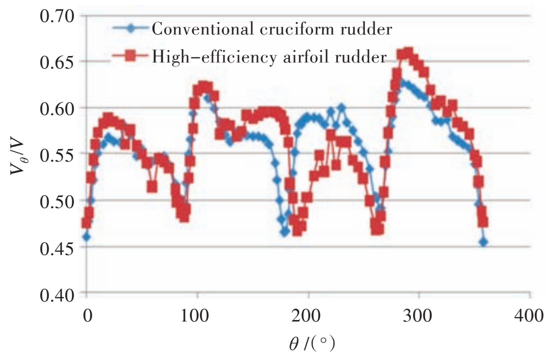

Fig.19 The comparison of wake at the radius of 0.6R

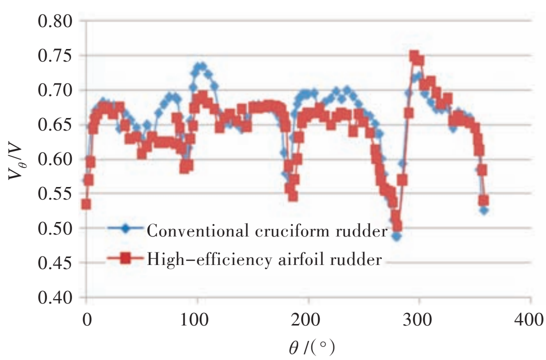

Fig.20 The comparison of wake at the radius of 0.8R

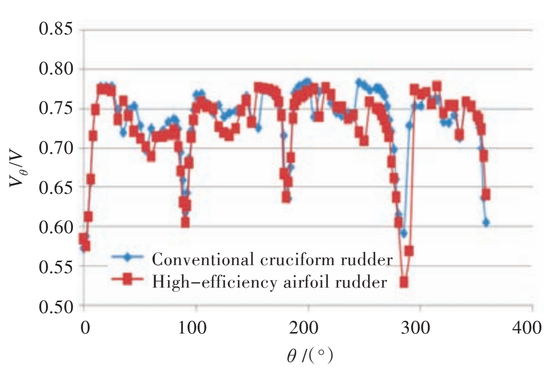

Fig.21 The comparison of wake at the radius of 1.0R

As can be seen from the figures, compared with the conventional rudder, the non-uniformity of wake field of the high-efficiency airfoil rudder is larger at all radii. Especially at the small radii, the non-uniformity increases by 60%–70%.

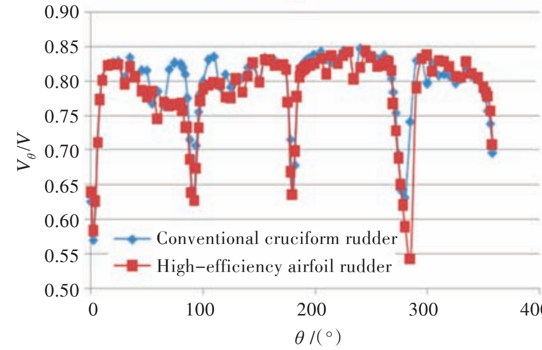

Fig.22 The comparison of wake at the radius of 1.2R

However, the large influence of high-efficiency airfoil rudder on wake field non-uniformity does not mean that the influence on the propeller noise is large. Because propeller has filtering effect, only when the harmonic frequency is equal to the harmonic component of wake field of the same number or the integral multiples of blades, the thrust pulsation, torque pulsation and tangential force pulsation of the propeller will be affected[10]. Therefore, the influence of rudder type on the propeller noise may be contrary to that of the non-uniformity of wake field, and the influence of rudder type on propeller noise is still to be further studied.

6 Conclusion

By the above calculation and comparative analysis it can be seen, for the same rudder area and aspect ratio, steerage of high-efficiency airfoil rudder has increased by more than 40% compared with conventional rudder in the whole range of rudder angle; but the influence on the total resistance of the hull is close at large rudder angle, less than 4% in error. The lifting efficiency by using the high-efficiency rudder is much more than the influence on the total resistance of the hull it brings, which has obvious advantages in improving the control efficiency, and good application prospects. The high-efficiency airfoil rudder can be applied to the bow rudder to reduce bow rudder scale, and for the application of stern rudder, its influence on propeller noise needs further study and discussion.

References

[1] YU X H, LIN J X. Analysis of the hydrodynamic forces on the stern-plane with assistant rudder of submarine [J]. Ship & Ocean Engineering, 2005(6): 28–30 (in Chinese).

[2] ZHU X Y, HUANG S, GUO C Y, et al. Design and performance of a skew rudder behind a propeller[J]. Journal of Harbin Engineering University, 2008, 29(2):

[Continued on page 70]

船舶碰撞机理三维解析法实现及恢复系数研究

刘俊峰[1,2], 胡志强[1,2]
1 上海交通大学 海洋工程国家重点实验室,上海 200240
2 高新船舶与深海开发装备协同创新中心,上海 200240

摘　要:[**目的**]采用解析方法分析船舶碰撞动力特性较为快速和准确,其中外部动力学分析十分重要。[**方法**]为此,运用MATLAB程序实现船舶碰撞外部机理三维简化解析方法,计算两艘船舶碰撞的动能损失,并与二维解析方法的计算结果进行比对。在实现船舶碰撞动能损失快速计算解析方法的基础上,讨论碰撞高度、角度和位置对动能损失的影响。此外,还研究碰撞场景对保守恢复系数的影响和保守恢复系数对动能损失的影响。[**结果**]结果表明:三维解析方法得到的动能损失小于二维解析方法,碰撞高度对于动能损失有明显的影响;简化解析方法中,对于碰撞角度大于90°的场景,恢复系数简单地取0并不安全。[**结论**]在今后的外部动力学分析中,为了使动能损失的计算值更加准确,可以使用三维解析方法代替二维解析方法。

关键词:船舶碰撞; 外部动力学; 三维解析法; 能量耗散; 恢复系数

[*Continued from page* 60]

126-129 (in Chinese).
[3] ZHU W W, WANG W F, GUO B C, et al. A practical symmetric aerofoil with high effectiveness[J]. Journal of Shanghai Jiaotong University, 1996, 30(10): 35-40 (in Chinese).
[4] CHEN W M. The effect of rudder forms on ship maneuverability[J]. Journal of SSSRI, 2002, 25(1): 40-43 (in Chinese).
[5] YU H X. The numerical simulation and experimental research of ichthyoid rudder' steady lift[D]. Harbin: Harbin Engineering University, 2003 (in Chinese).
[6] YANG J M. Prediction of performance of the shilling rudder behind a propeller[J]. Journal of Hydrodynamics, 1999, 14(2): 162-168 (in Chinese).
[7] MA Y C, LIN J X, ZHAO Y. 敞水舵水动力数值计算及分析[J]. China Water Transport, 2008, 8 (12): 1-3 (in Chinese).
[8] LI S Z, ZHAO F, YANG L. Multi-objective optimization for airfoil hydrodynamic performance design based on CFD techniques[J]. Journal of Ship Mechanics, 2010, 14(11): 1241-1248 (in Chinese).
[9] GIM O S, LEE G W. Flow characteristics and tip vortex formation around a NACA 0018 foil with an end plate [J]. Ocean Engineering, 2013, 60: 28-38.
[10] XIONG Z Y, SUN H X, ZHU X Q. 船尾伴流场与螺旋桨低频噪声相关性研究[C]//Proceedings of the Fourteenth Symposium on Ship Underwater Noise. Chongqing: Chinese Society of Naval Architects and Marine Engineers, 2013: 282-288 (in Chinese).

高效翼型舵在潜艇上的应用

周轶美, 张书谊, 卢溦, 何汉保
中国舰船研究设计中心,湖北 武汉 430064

摘　要:[**目的**]现代潜艇对操纵面设计的要求越来越高,使得设计者们需要不断研究新的舵型以提高操纵面的效率,而高效翼型舵是提高操纵面效率的有效措施之一。[**方法**]为此,在比较分析各种翼型优、缺点的基础上,提出一种优化的高效翼型舵,并采用数值计算的方法,比较分析潜艇上应用这种高效翼型舵与常规NACA舵的水动力特性和对尾部伴流场的影响规律,同时在拖曳水池中开展模型测力试验,发现试验结果与仿真计算结果一致性良好,误差不超过10%。[**结果**]研究结果表明:高效翼型舵的舵效比常规舵高40%以上,但对艇体总阻力的影响则与常规舵相当,不超过4%;采用高效翼型舵带来的升力效益要比其对艇体总阻力的影响大得多。[**结论**]表明高效翼型舵在提高操纵效率方面优势明显,有着较好的应用前景。

关键词:潜艇; 高效翼型舵; 水动力特性; 尾部伴流场